



## A METHOD FOR DETERMINING ASPERITY PARAMETERS PRODUCING SPECIFIC MAXIMUM GROUND MOTION

Masayuki YOSHIMI<sup>1</sup>, Takashi MIYATAKE<sup>2</sup> and Hiromichi HIGASHIHARA<sup>3</sup>

### SUMMARY

A method for determining fault parameters that provides a specific point with the maximum ground motion having specific dominant frequency is proposed. The time independent amplitude coefficient ( $C^{FS}$ ) and the rupture propagation amplification factor ( $C_{rup}$ ) are employed and their product  $C^{FS} * C_{rup}$  is utilized as a measure for determination of asperity allocation. The validity of this method has been examined by comparing its result with that of the grid searching procedure. Distributions of maximum velocity responses along a line perpendicular to the fault also have been examined with various dislocation parameters.

### INTRODUCTION

Recently, estimations of strong ground motions generated by specific seismic faults have widely been carried out. Obtained seismic intensity distributions or waveforms at some points have been opened to the public and they have been utilized for disaster mitigation planning or for the seismic design of structures.

Estimation of the maximum ground motion is of great concern in not only seismology but also earthquake engineering. In the seismic design, especially, the maximum ground motion that causes maximum response to the object structure is of great importance. To obtain that, strong motion simulations assuming fault parameters as random variables have been conducted (e.g. [1]). These approaches have disadvantage that a lot of calculation is necessary to obtain the maximum ground motion. The objective of this study is to develop a deterministic method to determine a fault model that generates maximum ground motion to a specific point.

### METHOD FOR STRONG MOTION CALCULATION

#### Far-field S-wave in full-space

To simulate the strong ground motion in full-space, the analytical Green's function of far-field S-wave [2] is employed. The displacement  $\mathbf{u}^{FS}$  in the time domain by a dislocation point source can be written as follows:

---

<sup>1</sup>National Institute of Industrial Safety, Japan, Email: yoshimi@anken.go.jp

<sup>2</sup>Earthquake Research Institute of Tokyo University, Japan

<sup>3</sup>Earthquake Research Institute of Tokyo University, Japan

$$\mathbf{u}^{FS}(\mathbf{x}, t) = \frac{\mu A [(\boldsymbol{\gamma} \cdot \mathbf{v}) \dot{\mathbf{u}} + (\boldsymbol{\gamma} \cdot \dot{\mathbf{u}}) \mathbf{v} - 2(\boldsymbol{\gamma} \cdot \mathbf{v})(\boldsymbol{\gamma} \cdot \dot{\mathbf{u}}) \boldsymbol{\gamma}]}{4\pi \rho \beta^3 r} \quad (1),$$

where  $\mu$  is the rigidity of the medium,  $A$  is the fault area,  $\dot{\mathbf{u}}$  is the dislocation velocity,  $\boldsymbol{\gamma}$  is the direction cosine,  $\rho$  is the density of the medium,  $\beta$  is the shear wave velocity and  $r$  is the source-receiver distance.

To synthesize the ground motion generated by a seismic fault, ground motions by regularly distributed point sources on the fault are summed up. Ground motion by a point source is obtained by convolution of the Green's function and the slip velocity function. The time series is summed in time domain taking rupture propagation effect into account.

The displacement is multiplied by 2.0 in order to consider the free surface effect.

### Ground motion in a half-space or in a medium with plane layers

To calculate the ground motion in a medium with plane layers, the discrete wave number method developed by Kohketsu [3] is used. With this method, body waves and surface waves emerged in the plane layered medium are calculated. After calculating Green's functions, the strong motion is synthesized in the same manner as described above.

## METHOD FOR ASPERITY PARAMETERS DETERMINATION

### Definition of coefficients

The time independent amplitude coefficient  $C^{FS}$ , amplitude of Green's function including in Eq. 1, can be written as follows:

$$C^{FS} = \frac{1}{|\dot{\mathbf{u}}| r} [(\boldsymbol{\gamma} \cdot \mathbf{v}) \dot{\mathbf{u}} + (\boldsymbol{\gamma} \cdot \dot{\mathbf{u}}) \mathbf{v} - 2(\boldsymbol{\gamma} \cdot \mathbf{v})(\boldsymbol{\gamma} \cdot \dot{\mathbf{u}}) \boldsymbol{\gamma}] \quad (2).$$

The  $C^{FS}$  for a fixed observer is dependent on both the source location and the source mechanism. Distributions of  $C^{FS}$  on fault planes are shown in Figure 1.

The direction of rupture propagation significantly affects the amplitude of the ground motion in the near fault area. Supposing that the rupture propagates toward one direction, an amplification factor of the ground motion by rupture propagation on the fault can be written as follows:

$$C_{rup} = \left( 1 - \frac{v_r}{\beta} \cos \theta \right)^{-1} \quad (3),$$

where  $v_r$  is the rupture velocity,  $\theta$  is the angle between the directions of the source-receiver and rupture propagation. In this formulation, the rupture fault is assumed to be propagating line-source and the distance between the fault and observer is assumed to be far; far-field approximation is employed.

### Asperity location determination

Since the ground motion generated by a propagating fault is the convolution of  $\mathbf{u}^{FS}(\mathbf{x}, t)$  and rupture propagation function, its strength or amplitude is related to the  $C^{FS} * C_{rup}$ . On the condition that both the asperity area and the rupture propagation manner are constant, the asperity  $S_\Omega$  that makes ground motion

maximum is supposed to be obtained through the following maximization problem of the  $C_i^{FS} * C_{rup}$  over the fault,

$$S_{\Omega} : \left\{ S_{asp} \subseteq S \mid \left| \int_{S_{asp}} C_i^{FS} C_{rup} dS \right| \rightarrow \max \right\} \quad (4),$$

where  $S_{asp}$  is the asperity.

### Asperity size determination

Waveforms of strong motions observed in the near fault region are characterized as pulse-like waves and pulse widths of them are related with sizes of their source asperities. In other words, the scale of asperity controls the dominant period/frequency of the strong ground motion around it. For the safety checking of a structure against ground motion, what is needed is the ground motion that makes the response of the structure largest. It is often the case with the response of a structure, only a few frequency components of the ground motion are important and of great concern. Therefore, the asperity size should be determined by the natural periods of the target structure. In this study, the following relation [4] between the dominant period or target period  $T_{target}$  and rupture parameters,

$$T_{target} = 2w \left( \frac{1}{v_r} - \frac{1}{\beta} \right) \quad (5),$$

where  $w$  is the width of the asperity, is employed.

### Rupture propagation in the asperity

The direction of rupture propagation strongly affects the amplitude of the ground motion in the near fault area. In the case that the rupture propagates to the very direction toward the observation point, namely the case of  $\theta = 0$  in Eq. 3, the amplitude of observed ground motion becomes its largest. Hence, in this study, the direction of rupture propagation is set to the orthogonal projection of the source to the receiver direction to the fault plane. The rupture is also set to propagate 1-dimensionally; in other words, the rupture-front is flat and is orthogonal to the direction of rupture propagation.

### Other fault parameters

It is assumed that the fault is rectangular and the asperity is square. The stress drop on the fault is assumed to be constant value. Then, the slip distribution is determined by the theoretical slip distribution on the rectangular crack obtained by Day [5] with slight modifications. Slip distributions for constant stress drops are shown in Figure 2. The slip velocity function of the fault dislocation produced by Nakamura and Miyatake [6] is employed. A shape of the function is shown in Figure 3. The rupture propagating velocity is supposed to be 80% of the shear wave velocity.

The maximum dislocation  $u_{max}$  on the fault [7][8] or asperity is obtained as follows:

$$u_{max} = \frac{\Delta\sigma}{\mu} w \quad (6),$$

where  $\Delta\sigma$  is the stress drop on the asperity.

## RESULTS AND DISCUSSION

### Full-space medium case

The  $C^{FS} * C_{rup}$  method described above is examined and compared with the grid searching method for a full-space medium. Properties of the medium are shown in Table 1. The target natural period is set to be 2.0 seconds and consequently the width of the square asperity is obtained to be 14 km with Eq. 5. The stress drop is supposed to be 10 MPa, making the maximum dislocation on the asperity 4.23 m by Eq. 6. The seismic fault assumed herein is 40 km long and extends to 20 km deep. Three dip angles are assumed; 30 deg., 60 deg and 90 deg., and two rake angles, 0 deg. and 90 deg. are employed. On the fault surface above the depth of 4 km from the ground, no dislocation is supposed. Single asperity is assumed in this examination.

In the  $C^{FS} * C_{rup}$  method, the maximization problem (Eq. 4) is firstly solved discretely and then the waveform is synthesized for the determined asperity location. On the other hand, in the grid searching, all the waveforms are firstly synthesized and responses of them are calculated and the maximum ground motion is selected. In each calculation, an asperity is arranged at intervals of 1 km along with both the strike direction and the dip direction, leading 54 arrangements of the asperity in the 90 deg. fault case, 144 arrangements in the 60 deg. case and 236 arrangements in the 30 deg. cases.

Shown in Figure 4 is the comparison of maximum pseudo velocity responses at the period 2.0 seconds obtained from grid searching with pseudo velocity responses for the ground motions synthesized using resultant asperity locations through Eq. 4. As a whole, the result of the  $C^{FS} * C_{rup}$  method is in good agreement with the grid searching result.

### Plane-layered media cases

The  $C^{FS} * C_{rup}$  method is examined not only in a half space but in a plane layered medium. Properties of those media are shown in Table 2 and Table 3, respectively. All the other parameters and conditions are same as those used in the full-space medium case but the limit depth of the fault dislocation, 2 km from the ground here. In both examination cases, the discrete wave number method is employed for calculation of waves.

In Figure 5, pseudo-response distributions of the fault normal ground motions synthesized with the 60 deg. dipped and 0 deg. rake fault in the half-space medium are shown. These data are obtained through the grid searching procedure. The number at the upper left corner of each figure indicates the distance of the observation point from the fault line. The observation point is located on the strike=0 km plane. Each bar in the figure is drawn at the center of each asperity location. The asperity location affects the intensity of the ground motion.

Shown in Figure 6 and Figure 7 are the comparisons of maximum pseudo velocity responses at the period 2.0 seconds obtained by the  $C^{FS} * C_{rup}$  method (Eq.4) with those obtained by the grid searching in the half space and in the plane-layered medium, respectively. In the cases of high dip angle faults, results of the  $C^{FS} * C_{rup}$  method are in good agreement with those of the grid searching in both media. In the cases of 30 deg. dipped fault, the  $C^{FS} * C_{rup}$  method sometimes underestimates maximum ground motions. It is because that only the contribution of far-field S wave is considered in the  $C^{FS} * C_{rup}$  method and that contributions of other wave components are relatively large in some of the 30 deg. dip fault cases. Even in the case of the 30 deg. dipped fault, maximum values at the near fault area (less than 5 km from the fault line) are successfully obtained with the method.

## CONCLUSIONS

In the present work the method for determining asperity parameters using amplitude of analytical Green's function and amplification factor by rupture propagation has been developed and examined. Through the examination in the full space medium and in plane-layered media, maximum ground motions have

successfully been detected with the  $C^{FS} * C_{rup}$  method. Distributions of maximum velocity responses along perpendicular to the fault for various fault geometries have been examined. The advantage of the method is time independency; all the terms contained in the measure  $C^{FS} * C_{rup}$  proposed herein are independent of time. It can be concluded that the  $C^{FS} * C_{rup}$  method is efficient method to determine the location of the asperity for the estimation of the maximum ground motion.

## REFERENCES

1. Megawati, K. and TC. Pan (2002): Prediction of the maximum credible ground motion in Singapore due to a great Sumatran subduction earthquake: the worst scenario, *Earthquake Engng. Struct. Dyn.*, 31, 1501-1523.
2. Aki, K. and P. G. Richards (1980): *Quantitative Seismology*, W.H. Freedman and Company.
3. Kohketsu, K. (1985): The extended reflectivity method for synthetic near-field seismograms, *J. Phys. Earth*, 33, 121-131.
4. Miyatake, T. (1998): Generation mechanism of strong ground motion pulse near the earthquake fault, *Zisin (J. Seism. Soc. Japan)*, 51, 161-170 (in Japanese).
5. Day, M.S. (1982): Three-dimensional finite difference simulation of fault dynamics: rectangular faults with fixed rupture velocity, *Bull. Seis. Soc. Am.*, 72, 705-727.
6. Nakamura, H. and T. Miyatake (2000): An approximate expression of slip velocity time functions for simulation of near-field strong ground motion, *Zisin (J. Seism. Soc. Japan)*, 53, 1-9 (in Japanese).
7. Knopoff, L. (1958): Energy release in earthquakes, *Geophys. J.*, 1, 44-52.
8. Chinnery, M.A.(1968): *Theoretical fault models*, Publication of the dominion observatory, 211-223.

**Table 1: Full space model**

Thick (km)	$\alpha$ (km/s)	$\beta$ (km/s)	$\rho$ (g/cm <sup>3</sup> )	Qp	Qs
Inf.	6.00	3.5	2.7	-	-

**Table 2: Half space model**

Thick (km)	$\alpha$ (km/s)	$\beta$ (km/s)	$\rho$ (g/cm <sup>3</sup> )	Qp	Qs
Inf.	6.00	3.5	2.7	600	300

**Table 3: Plane layer model**

Thick (km)	$\alpha$ (km/s)	$\beta$ (km/s)	$\rho$ (g/cm <sup>3</sup> )	Qp	Qs
0.10	2.50	1.00	2.10	60	20
0.40	3.20	1.80	2.10	100	30
4.50	5.50	3.20	2.60	600	300
Inf.	6.00	3.46	2.70	600	300

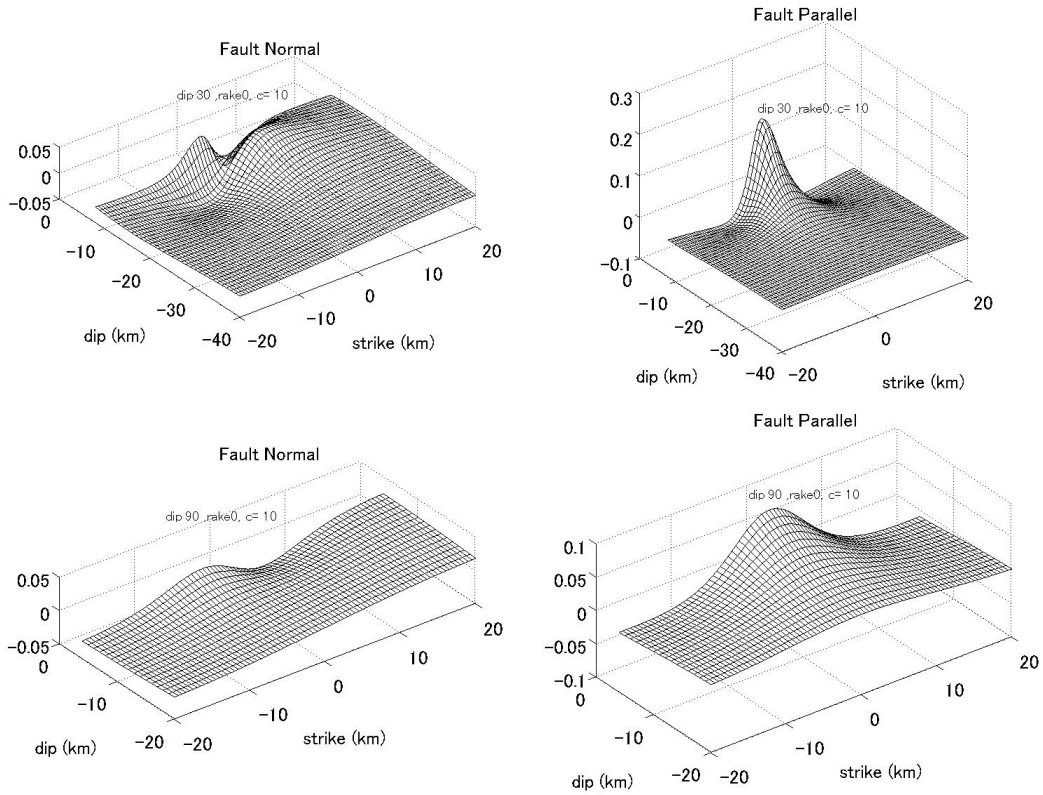


**Figure 1. Distributions of  $C^{FS}$  on fault planes, calculated for 30 deg. dip angle (top) and 90 deg. dip angle (bottom), respectively (10 km from fault lines, rake = 0 deg. in common).**

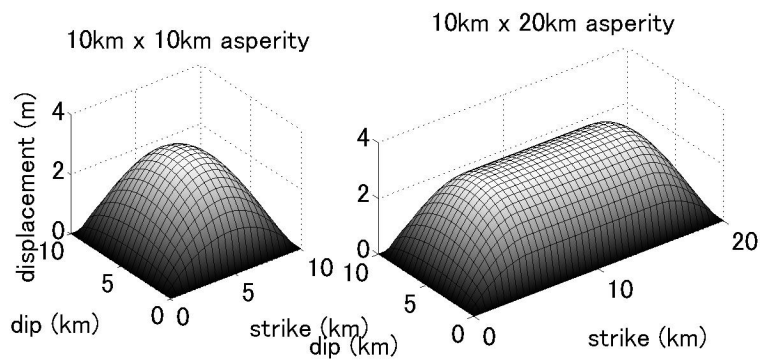


**Figure 2. Dislocation distributions on fault planes ( $\Delta\sigma = 10$  [MPa],  $w = 10$  km,  $\mu=33.075$  GN/m<sup>2</sup>)**

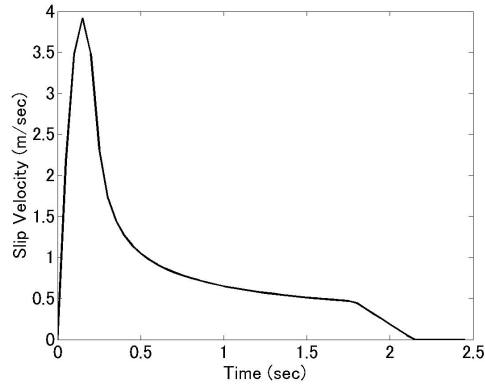


Figure 3. Slip velocity time function (Nakamura and Miyatake, 2000)

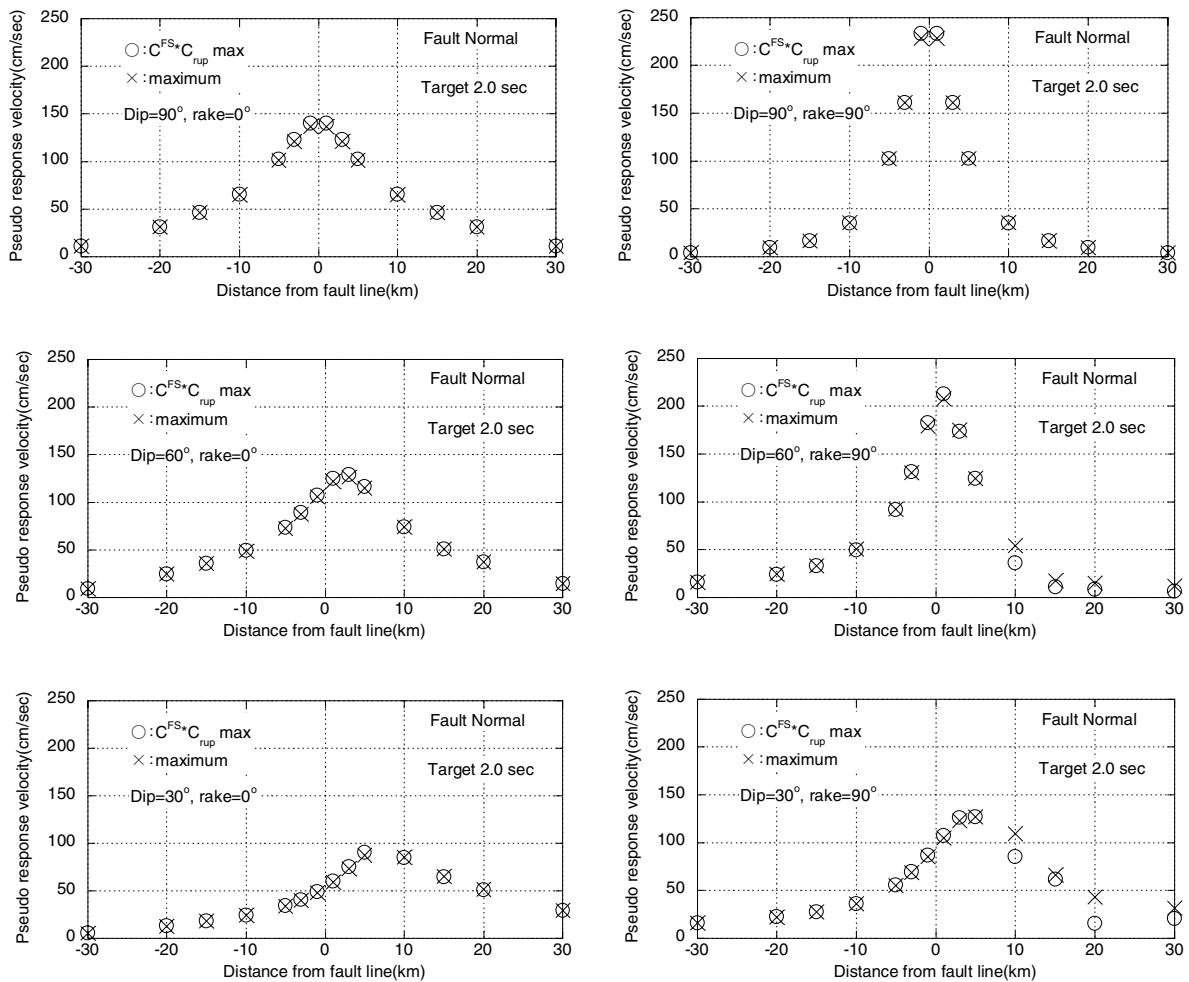
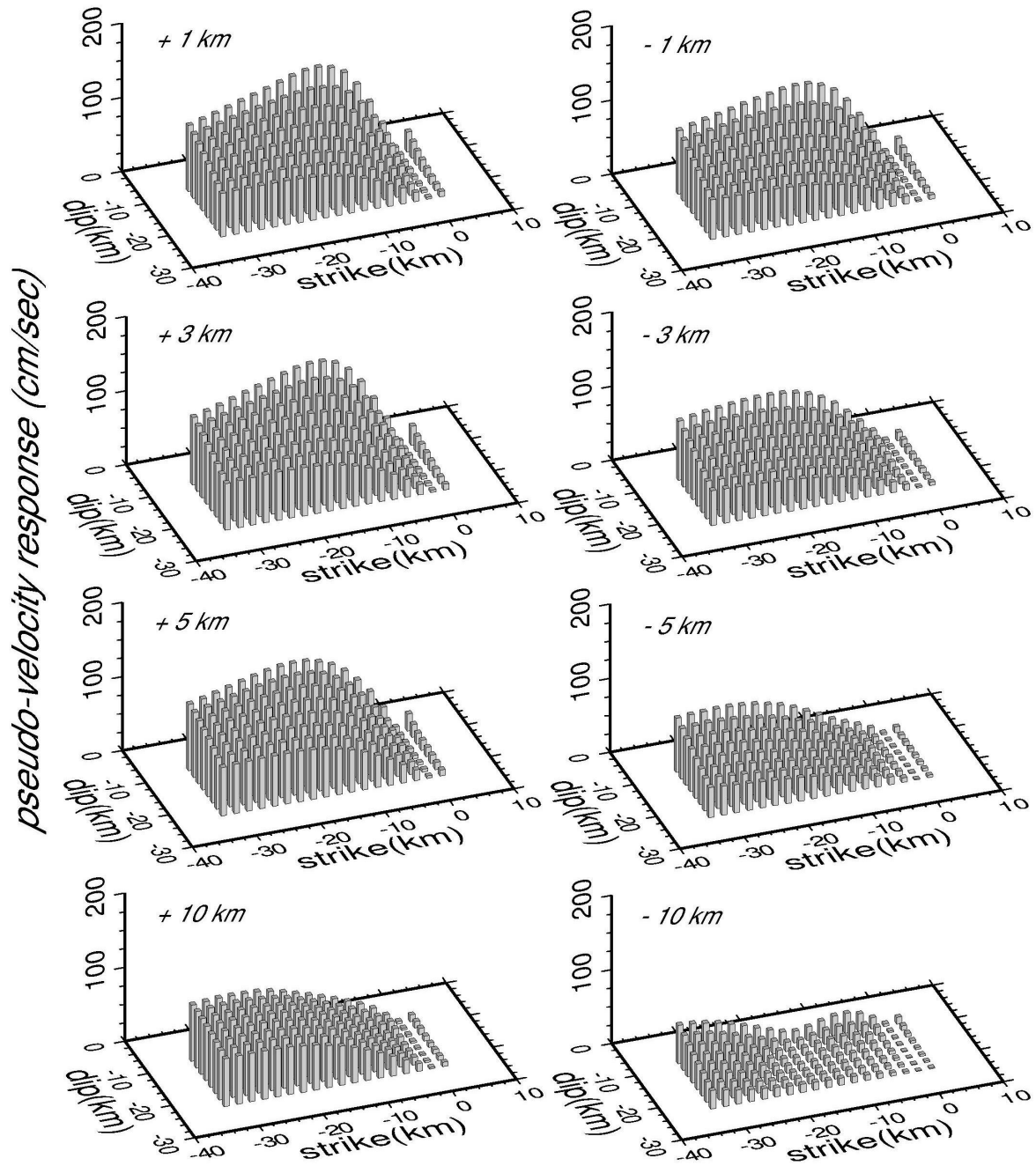
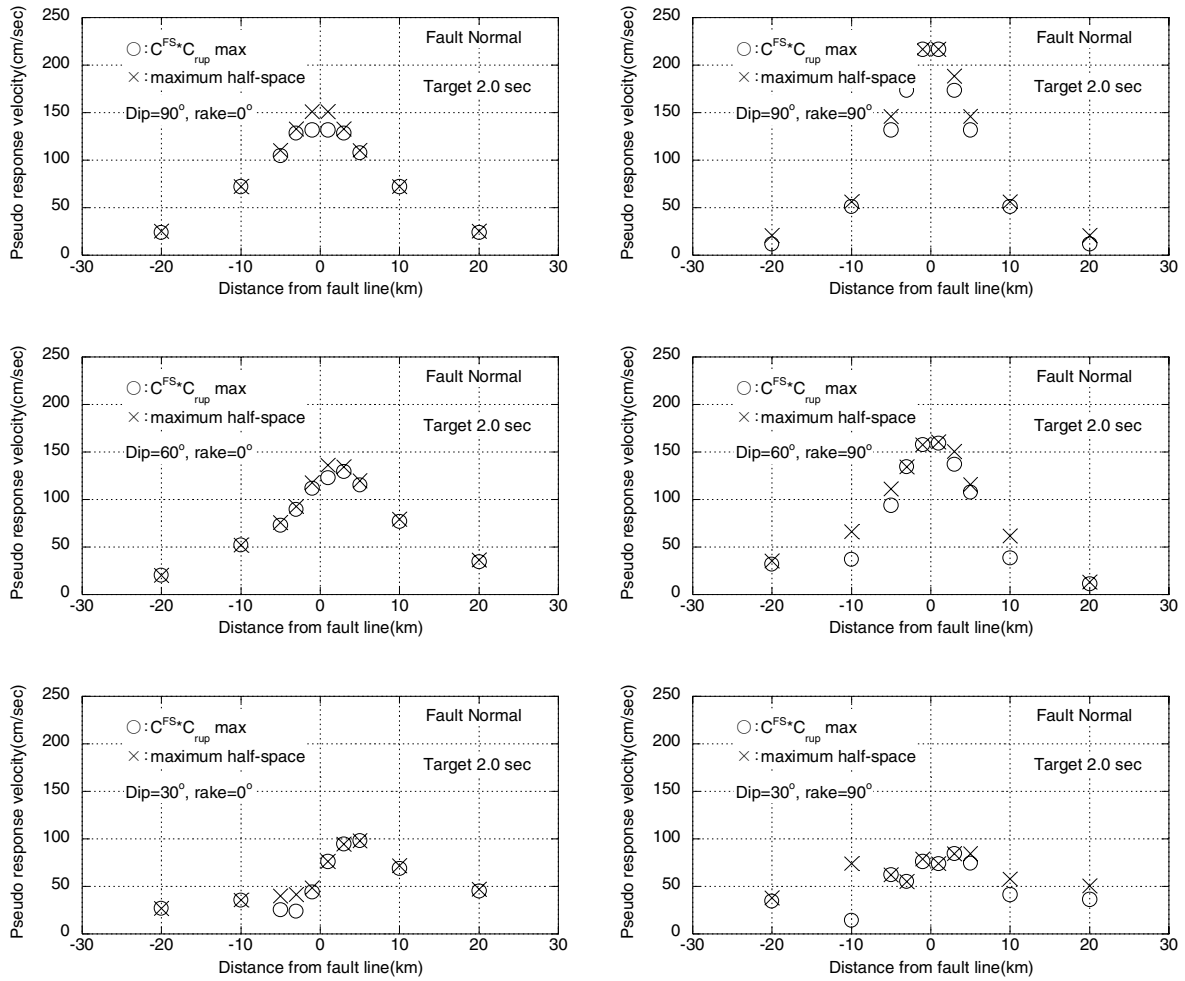


Figure 4. Full-space case of comparisons of maximum responses obtained by the  $C^{FS} * C_{rup}$  method (crisscrosses) and by the grid searching (circles), pseudo velocity responses at period 2.0 sec. in the fault normal direction. The minus in the distance from the fault indicates that the observation point is located in the footwall, and vice versa.

*Dip 60 deg., rake 0 deg., Fault Normal, 2.0 sec. response*



**Figure 5. Pseudo-response distributions of the fault normal ground motions synthesized with the 60 deg. dip angle and 0 deg. rake angle fault in the half-space medium. Distance of the observation point from the fault line is shown at the upper corner of each figure. The observation point is located on strike=0km plane. Each box stands on at the center of each asperity location.**



**Figure 6. Half-space cases of comparison of maximum responses obtained by the  $C^{FS} * C_{rup}$  method (crisscrosses) and by the grid searching (circles), pseudo velocity responses at the period 2.0 sec. in the fault normal direction.**

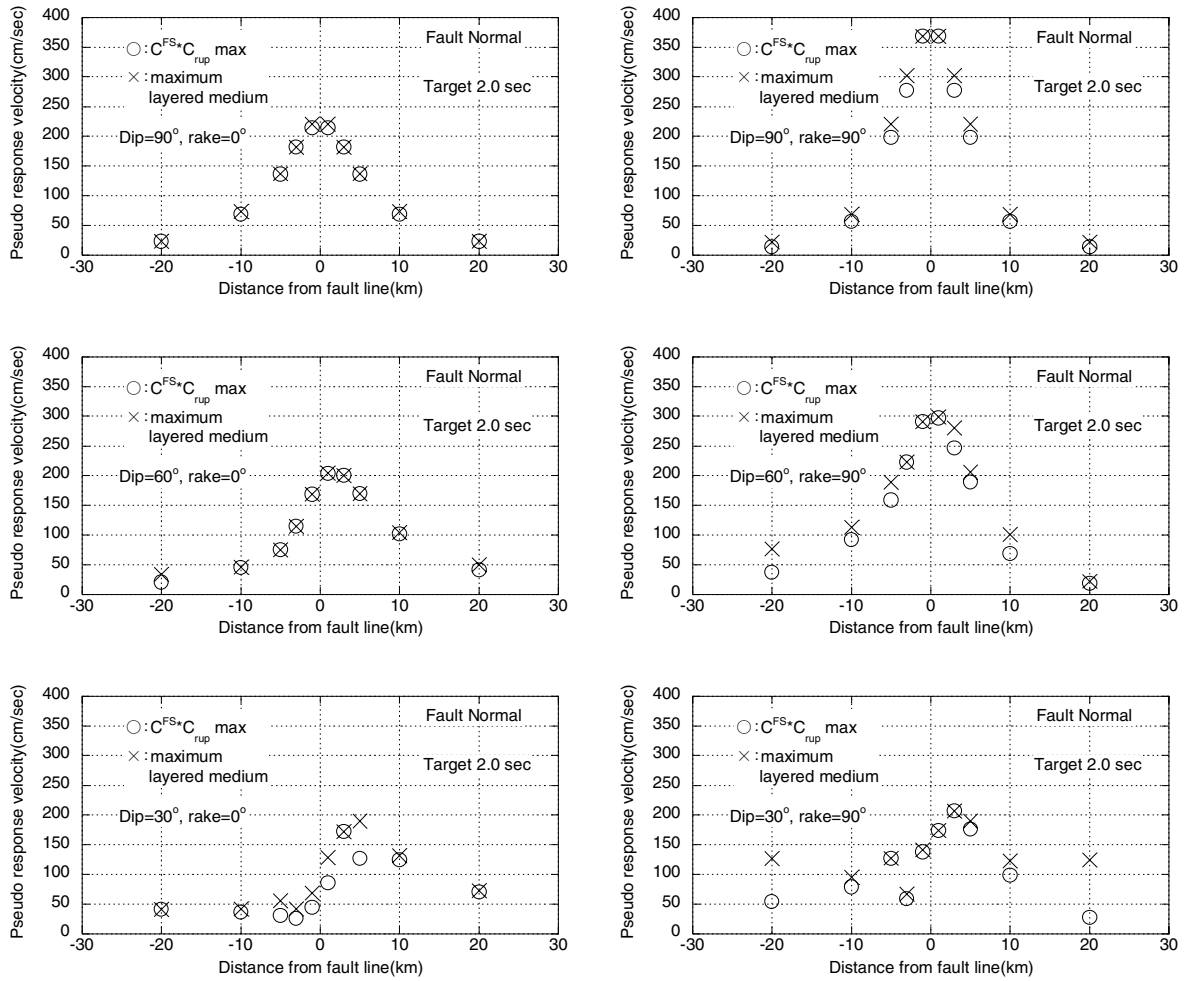


**Figure 7. Plane layered medium cases of comparison of maximum responses by the  $C^{FS} * C_{rup}$  method (crisscrosses) and by the grid searching (circles), pseudo velocity responses at period 2.0 sec. in the fault normal direction.**